^{2}H NMR Investigations of the Hexadecane/Urea Inclusion Compound

Judith Schmider and Klaus Müller*

Institut für Physikalische Chemie, Universität Stuttgart, Pfaffenwaldring 55, D-70569 Stuttgart, Germany

Received: August 19, 1997; In Final Form: November 18, 1997

The molecular behavior of selectively deuterated *n*-hexadecane in the urea inclusion compound is studied between 100 and 290 K by means of dynamic ^{2}H NMR spectroscopy employing line shape studies and spin−spin and spin−lattice relaxation experiments. Particular emphasis is given to the changes of the guest molecule behavior close to a solid−solid phase transition occurring at lower temperatures which is accompanied by a distortion of the urea lattice. It is demonstrated that spin−lattice relaxation experiments are of particular help for the evaluation of the chain dynamics in such systems. A comprehensive computer analysis of the available experimental data could provide a detailed picture of the hexadecane chains in the low-temperature phase and above the solid−solid phase transition. In the low-temperature phase the alkyl chains are found to undergo fast but restricted rotational motions (rate constant ca. 10^7 s^{-1}). In addition, intramolecular *trans*−*gauche* isomerizations and methyl group rotation contribute to the spin relaxation of the alkane chain ends. In the high-temperature phase the alkyl chains rotate rapidly (rate constant ca. 10^{10} s^{-1}) and almost unrestricted around the channel long axis, giving rise to a dynamic (rotational) disorder of the embedded alkyl chains. It therefore is concluded that the phase transition can be assigned to a (dynamic) order−disorder transition. The alkane chains furthermore are found to be perfectly aligned with respect to the urea channel long axis. At the same time, they exhibit an internal flexibility gradient toward the chain ends. The conformational order significantly is altered at the phase transition. Thus, the *trans* population in the low-temperature phase is given by $p_t = 0.7$ while in the high-temperature phase a value of $p_t = 0.95$ has been derived.

Introduction

Urea is known to form inclusion compounds (UICs) with various long-chain hydrocarbons.[1,2] The urea host structure consists of a hydrogen-bonded arrangement of urea molecules that build up a honeycomb-like framework of one-dimensional, parallel, nonintersecting channels of "infinite" length and an inner diameter of ca. 5.25 Å.[3] At the same time, the channel diameter presents the discriminator for the guest molecules that are incorporated. It turns out that only linear, branched, or functionalized hydrocarbons with typical substituents such as methyl and ethyl groups or halogen atoms fit into the urea channels. The spatial constraints imposed by the rigid host matrix also favor a linear and extended conformation of the incorporated guest molecules.

From former calorimetric,[4] X-ray,[5−10] and spectroscopic[11−16] studies it is known that UICs with *n*-alkanes undergo a solid−solid phase transition. The corresponding transition temperatures increase monotonically with the length of the alkane guest molecules and display a characteristic odd−even effect as function of the number of methylene chain segments. X-ray investigations have shown that the high-temperature phase—being stable at room temperature—is characterized by a hexagonal symmetry of the urea channels with stretched paraffin chains in an almost *all-trans* conformation.[5−10] The experimental data gave rise to an average structure that is generated by a fast rotational motion of the alkane chains around the channel long axis. At the solid−solid phase transition the channels become slightly narrower. The hexagonal structure of the urea framework now is distorted and is transformed to an orthorhombic structure. At the same time, the rapid rotational motions of the *n*-alkanes are assumed to be quenched. The guest molecules thus lose their rotational freedom and occupy specific positions within the urea host lattice. In this connection, several papers have been published that deal with the theoretical description of the solid−solid phase transitions in UICs with *n*-alkanes.[17−19]

Dynamic NMR techniques have been used extensively for the evaluation of dynamic processes in molecular solids.[20−25] Among these, ^{2}H NMR methods have demonstrated their particular suitability for the characterization of the guest dynamics in inclusion compounds.[25−28] Depending on the dynamic range various experimental techniques, such as line shape experiments and spin−lattice relaxation measurements, have been applied. Up to now, several ^{2}H NMR studies on single-crystal[26,29,30] or powder samples[31,32] of UICs exist with selectively or perdeuterated *n*-alkanes of different chain lengths ($n = 16, 19$). Although experimental data have been published for both the low- and high-temperature phases of UICs, so far, the experimental analysis mainly was focused on the high-temperature phase. Various motional models have been proposed for the UIC with nonadecane which should be responsible for the spin−lattice relaxation of the alkane chains in the high-temperature phase.[26] A more recent single-crystal study[30] of the UIC with nonadecane primarily dealt with the conformational properties in the high-temperature phase and the changes at the transition to the low-temperature phase. However, quantitative data on the latter topic have not been provided.

In the following we present a ^{2}H NMR investigation of the hexadecane/urea inclusion compound for a temperature range between 100 and 290 K where particular emphasis is given to the molecular behavior of the guest molecules in the low-temperature phase and in the vicinity of the solid−solid phase transition. During the present study UIC samples with two selectively deuterated hexadecanes are examined (Figure 1).

S1089-5639(97)02703-5 CCC: $15.00
Published on Web 01/22/1998

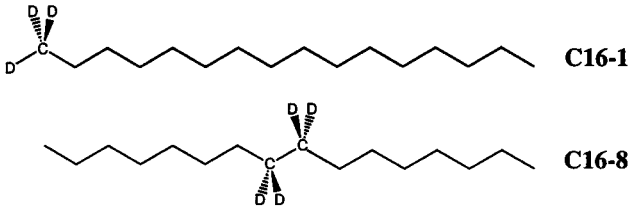

Figure 1. Structures of the selectively deuterated hexadecanes used during the present ^{2}H NMR study.

Sample **C16−8** is labeled at the two central carbons while sample **C16−1** is bearing a perdeuterated methyl group. The quantitative analysis of the line shape and relaxation experiments provides a detailed insight into the chain dynamics—which exhibit various internal and overall contributions—as function of temperature and UIC phase. Moreover, the combined analysis of both labeled compounds yields information about the changes in conformational flexibility across the hydrocarbon chains and the overall chain order within the two UIC phases.

Experimental Section

Materials. Urea was purchased from Aldrich Chemicals and was used without further purification. Selectively deuterated *n*-hexadecanes have been prepared according to the following procedures:

*(i) n-Hexadecane-1,1,1-d_3 (**C16−1**).* Hexadecanoic acid ($C_{15}H_{31}COOH$) was reduced with $LiAlD_4$ employing standard procedures. The obtained hexadecanol-*1,1-d_2* was transformed into its bromide by the reaction with sodium bromide in dilute sulfuric acid. The bromide was transferred to the Grignard compound, followed by the addition of D_2O. The product *n*-hexadecane-*1,1,1-d_3* was purified by destillation.[33]

*(ii) n-Hexadecane-8,8,9,9-d_4 (**C16−8**).* Octanoic ethyl ester ($C_7H_{15}COOCH_2CH_3$) was reduced with $LiAlD_4$. The corresponding bromide was obtained by the reaction of octanol-*1,1-d_2* with sodium bromide in an aqueous solution of sulfuric acid. In a copper/lithium-catalyzed coupling reaction the 1-bromo-octane-*1,1-d_2* was converted into n-hexadecane-*8,8,9,9-d_4*. The product was purified by destillation.[34]

Urea Inclusion Compounds. The urea inclusion compounds were prepared by precipitation of the selectively deuterated *n*-hexadecanes from a hot, saturated solution of urea in methanol. The white needles were filtered, washed with 2,2,4-trimethylpentane, and dried.[1,5] Calorimetric studies were carried out with a Netzsch DSC 200 differential scanning calorimeter.

NMR Studies. All ^{2}H NMR experiments were done at 46.07 MHz on a Bruker CXP 300 spectrometer interfaced to a Tecmag spectrometer control system. The experimental ^{2}H NMR spectra were obtained using the quadrupole echo sequence $(\pi/2)_x-\tau_1-(\pi/2)_y-\tau_2$ with $\pi/2$ pulses of 1.8−2.0 μs and a pulse spacing of $\tau_1 = \tau_2 = 30$ μs. The same pulse sequence could be used for the determination of spin−spin relaxation times (T_2) by the variation of $\tau_1 = \tau_2$. Spin−lattice relaxation times (T_{1Z}) were measured by a modified inversion recovery sequence, $\pi-\tau_r-(\pi/2)_x-\tau_1-(\pi/2)_y-\tau_2$, using the quadrupole echo sequence for signal detection and varying the interval τ_r. In these experiments a composite pulse was used instead of the inversion π pulse which is given by $[\pi/2]_\phi[\pi/2]_{\phi\pm\pi/2}[\pi/2]_\phi$, with appropriate phase cycling ($\phi = 0$, $\pi/2$, π, and $3\pi/2$).[35] Recycle delays were chosen to be at least 5 times the spin−lattice relaxation time T_{1Z}. The number of scans varied between 200 and 1024. The sample temperature during the variable temperature experiments was controlled with a Bruker BVT 1000 temperature control unit. Generally, the temperature stability was found to be within ±1 K.

Data Processing and Simulations. FORTRAN programs have been developed that describe the behavior of an $I = 1$ spin system during the corresponding line shape and relaxation experiments.[36] The simulation programs are very general and account for various types of molecular motion of the system under investigation (see Appendix). The theoretical line shapes and relaxation times are obtained by a numerical diagonalization of the corresponding relaxation matrixes using standard software packages.[37] The fitting of the experimental spectra has been done by superimposing the experimental and theoretical spectra. The final (best fit) spectra were obtained by taking into account the overall line shape as well as the relative amplitudes in case of partially relaxed spectra. Both the simulations and data processing of the experiments were performed on SUN workstations using the NMR1 and Sybyl/Triad software packages (Tripos, St. Louis, MO).

Results

Two samples of the urea inclusion compound with hexadecane have been studied between 100 and 290 K: (i) sample **C16−8** with hexadecane deuterated at the two central carbons and (ii) sample **C16−1** with hexadecane deuterated at the terminal methyl group. Dynamic ^{2}H NMR spectroscopy is a well-established technique to evaluate the motional and structural characteristics on a molecular level. In recent years this technique has shown its particular potential during the characterization of quite different chemical systems such as liquid crystals, polymers, biological membranes, or inclusion compounds.[20−25] Taking into consideration the various experimental techniques available, dynamic ^{2}H NMR spectroscopy can be used to study molecular processes over several orders of magnitude. The particular situation in ^{2}H NMR spectroscopy is due to the fact that the spin Hamiltonian is dominated by the quadrupolar interaction with the main interaction axis along the C−^{2}H bond. As a result, the analysis of such ^{2}H NMR experiments can provide detailed information about the actual molecular characteristics of the systems under investigation. The corresponding ^{2}H NMR spectra and the spin−spin relaxation times T_2 are sensitive to molecular processes with rate constants in the order of the quadrupolar coupling constant, i.e., between 10^4 and 10^8 s^{-1}. Likewise, spin−lattice relaxation measurements[38] can be used to study very fast motions with rate constants between 10^8 and 10^{11} s^{-1}. Very slow motions (rate constants $10^{-1}-10^2$ s^{-1}) are accessible employing 2D exchange[39] and hole-burning experiments.[40]

To begin with, we discuss the results obtained for sample **C16−8**. Figure 2 shows representative ^{2}H NMR spectra of this sample between 100 and 290 K covering both the low- and high-temperature phase. It is quite obvious that the solid−solid phase transition at 156 K has a strong impact on the corresponding ^{2}H NMR spectra. In the low-temperature phase at 103 K a typical, almost axial symmetric "rigid limit" spectrum is detected. The experimental splitting between the perpendicular singularities of 119 kHz is close to completely immobile guest molecules. Upon heating within the low-temperature phase (100 K < T < 156 K) the ^{2}H NMR spectra display a gradual increase in spectral biaxiality ($\eta > 0$). Above the phase transition, again axial symmetric powder spectra are observed which now are reduced in spectral width by a factor of $^1/_2$ (experimental splitting at 173 K: 60 kHz).

These findings can be understood by assuming for the low-temperature phase a fast but very restricted rotational motion (see Figure 3) of the hexadecane chains around their *all-trans* axes. The theoretical spectra, also given in Figure 2, have been

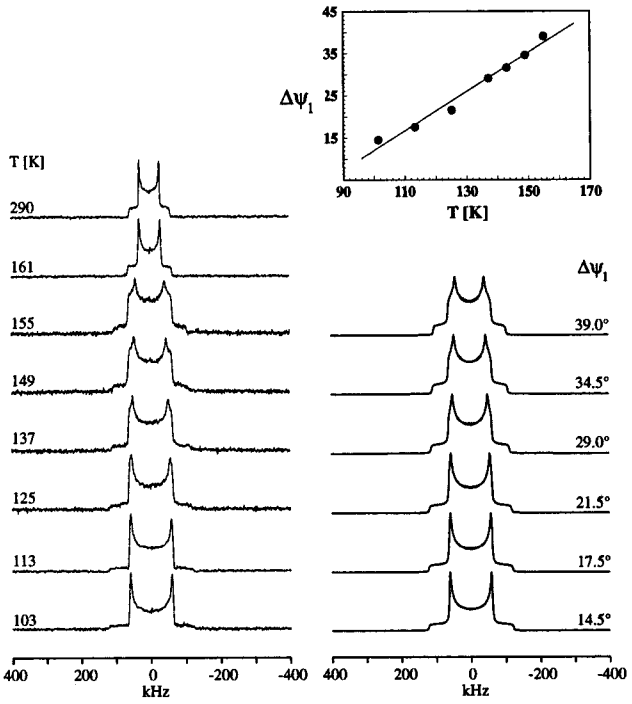

Figure 2. Experimental and simulated spectra of **C16−8**. Simulations for the low-temperature phase spectra were carried out assuming a fast two-site jump motion with the jump angles $\Delta\psi_1$ given in the figure.

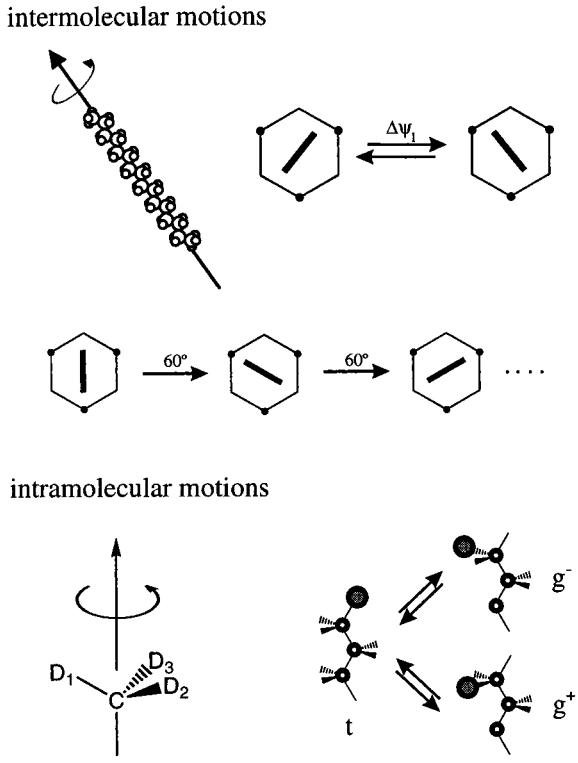

Figure 3. Proposed inter- and intramolecular motions of hexadecane chains within the urea channels.

obtained by modeling the chain motions with a jump process between two equally populated sites and a *trans* population for the inner segment of $p_t = 1.0$. The other simulation parameters are given in Table 1 while the various coordinate systems used for the simulation of the NMR experiments are summarized in Figure 4. The rate constants for the simulations have been chosen to be in the fast exchange limit. Inspection of Figure 2 suggests that the chosen motional model is appropriate to describe the experimental spectra. It is interesting to note that

TABLE 1: Simulation Parameters Used for the Calculation of the NMR Experiments

sample	C16−1	C16−8
quadrupolar coupling constant[a] e^2qQ/h (kHz)	167	167
residual line width[b] $1/(\pi T_2^0)$ (kHz)	3.0 (1.0)	3.0 (1.0)
transformation angles[c] (deg)		
ϕ_1	0.0; 0.0; 0.0	0.0
θ_1	−144.75; 90.0; 90.0	0.0
ψ_1*[d]	0.0; −54.75; 54.75	0.0
ϕ_2	0.0; 0.0; 0.0	0.0
θ_2	70.5; 70.5; 70.5	90.0
ψ_2	0.0; 120.0; 240.0	0.0

[a] Asymmetry parameter $\eta = 0$. [b] Values for low and high (in parentheses) temperature phase. [c] Euler angles ϕ_1, θ_1, ψ_1, relating the molecular axis and channel axis system; Euler angles ϕ_2, θ_2, ψ_2, relating the magnetic principal axis and the molecular axis system (see Figure 3b). For **C16−1** three sets of angles ϕ_1, θ_1, ψ_1 are given which refer to the *trans*, *gauche*$^+$, and *gauche*$^-$ sites. The three sets of angles ϕ_2, θ_2, ψ_2 for **C16−1** refer to three sites used to describe methyl group rotation. [d] Chain rotation is considered by taking $\psi_1(n) = \psi_1^* + n\Delta\psi_1$ where n and $\Delta\psi_1$ refer to the number of sites and jump angle between neighboring sites.

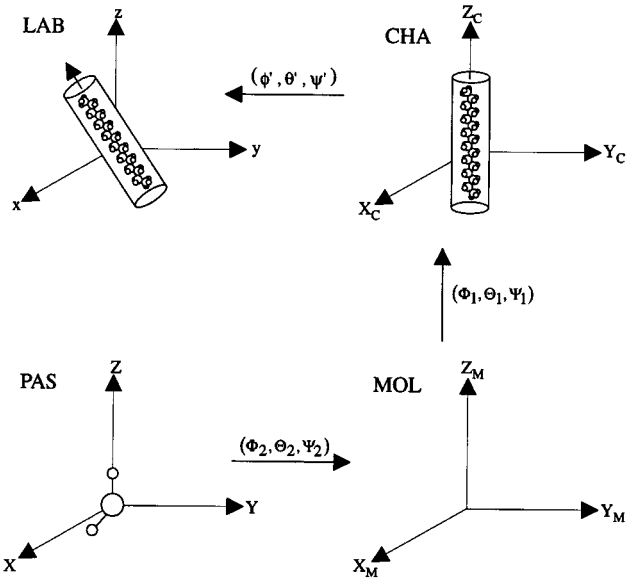

Figure 4. Coordinate systems and transformation angles used for the present NMR data analysis (LAB: laboratory axis system, defined by magnetic field direction; CHA: channel axis system, defined by channel long axis; MOL: molecular axis system, defined by internal axis like C2−C3 bond; PAS: principal axis system, defined by the C−^{2}H bond).

there exists an almost linear relationship between the jump angle and the sample temperature. According to the experimental analysis, the jump angle varies between 14.5° at 103 K and 39.0° close to the solid−solid phase transition. The restriction of the overall chain motion in the low-temperature phase certainly can be traced back to the low symmetry of the local, molecular environment; due to the distorted hexagonal urea channels, only small deviations from the equilibrium position are allowed. It should be noted that such biaxial spectra also can be obtained by assuming reorientational jumps between inequivalent sites, i.e., sites of different relative populations. For example, the consideration of a jump angle of 90°—which reflects the angle separation between adjacent minima in the potential energy curve of the low-temperature phase[6]—and relative populations for the major site between 0.97 and 0.89 yields the same biaxial spectra, as shown in Figure 2.

In quite contrast, in the high-temperature phase the urea

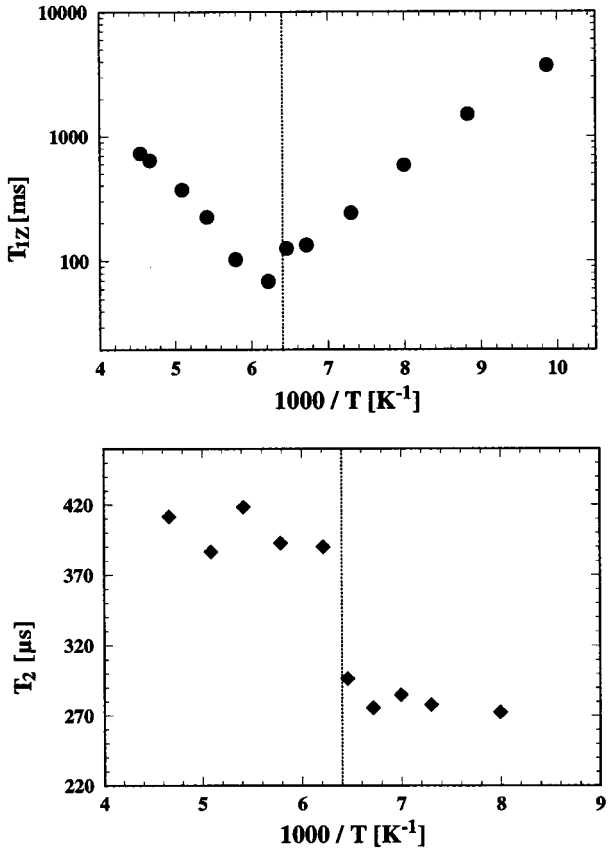

Figure 5. Experimental T_{1Z} and T_2 relaxation data of **C16−8**. The phase transition is indicated by the dashed line.

channels exhibit a hexagonal symmetry and a slightly larger cross-sectional area. As a result, the hexadecane chains now can undergo almost unhindered rotations about their long axes, which is in agreement with earlier investigations of the high-temperature phases of other UICs. It is interesting to note that the spectral splittings remain almost constant up to 290 K (splitting 59.8 kHz), which implies the absence of a pronounced wobble motion perpendicular to the chain long axis.

Further information about the rate constants and the kinetic parameters can be obtained from the analysis of relaxation experiments. In Figure 5 the spin−spin and spin−lattice relaxation data are given for sample **C16−8**. These data refer to the overall values of the powder sample which have been derived from the amplitudes of the corresponding free induction decays as function of the variable pulse interval $\tau_1 = \tau_2$ (quadrupole echo experiment) and τ_r (inversion recovery experiment), respectively. Thus, the experimental T_2 data exhibit an increase with temperature along with a discontinuity at the solid−solid phase transition which is expressed by an abrupt change in T_2 from 300 to 390 μs. Again, these findings suggest that different molecular processes are responsible for spin−spin relaxation in the low- and high-temperature UIC phases. It turned out that for the UIC studied here the spin−lattice relaxation data are much more informative than the spin−spin relaxation data (see next paragraph). Therefore, we refrained from a quantitative analysis of the experimental T_2 data.

The experimental T_{1Z} relaxation curve of Figure 5 again indicates the presence of different motional processes in the low- and high-temperature phase. This can be taken immediately from the fact that the T_{1Z} curve displays different slopes (absolute values) for the low- and high-temperature branches. It is observed that for the low-temperature phase the T_{1Z} values decrease with increasing temperature. The responsible relaxation process thus is characterized by rate constants being smaller than the Larmor frequency. At the solid−solid phase transition a discontinuity of the T_{1Z} curve can be detected along with a change of the sign of the slope. In the high-temperature phase the dominant relaxation process occurs in the extreme fast exchange limit with rate constants being larger than the Larmor frequency.

The analysis of such experimental overall T_{1Z} data usually is done by a comparison with theoretical T_{1Z} curves which are derived on the basis of a suitable motional model. In this connection, particular emphasis is given to the absolute value at the T_{1Z} minimum. Deviations between the experimental and theoretical T_{1Z} minima are taken as an indicator for the quality of the model assumption. However, one should be aware of the fact that accidentally different motional models might result in quite similar T_{1Z} relaxation curves. Thus, for some cases the exclusive consideration of T_{1Z} data might result in an ambiguous analysis.

Theroretical T_{1Z} curves have been derived by assuming a two-site jump process at various jump angles (not shown). Such simulations clearly show that the jump angle has a significant influence on the absolute values of T_{1Z}. From this, the rate constants for the restricted chain motion in the low-temperature phase can be derived with the known jump angles from the analysis of the quadrupole echo spectra (see above, Figure 2). As will be outlined below, the consideration of the experimental T_{1Z} anisotropy can provide further information about the quality of the model assumption used for the T_{1Z} data analysis.

Likewise, the high-temperature phase can be analyzed with the consideration of theoretical T_{1Z} curves obtained for unrestricted chain motions. Here, two possibilities exist: (i) 6-fold jumps ($2\pi/6$ jumps) between equally populated sites of the hexadecane chains around the channel axis or (ii) the mechanism of a "free" rotation (rotational diffusion) of the chains within the urea channel. Since both motional modes give rise to very similar experimental curves (only the T_{1Z} minima are slightly shifted), it is not possible to distinguish between these types of motion on the basis of the present experimental T_{1Z} values.

Previous relaxation studies on other molecular solids[41−44] have demonstrated that the T_{1Z} anisotropy[38] is a reliable tool for the determination of the underlying molecular processes that are responsible for spin relaxation. It should be mentioned that generally the T_{1Z} anisotropy depends on both the type of motion and the actual rate constant. Thus, the anisotropy might be different for motions being faster or slower than the Larmor frequency, i.e., motions above or below the T_{1Z} minimum.

In Figures 6 and 7 partially relaxed ^{2}H NMR spectra for the low- and high-temperature phase are given which were obtained by the inversion recovery experiment as function of the pulse spacing τ_r. Inspection of the experimental spectra reveals that different T_{1Z} anisotropies exist in the high- and low-temperature phases. This can be attributed to the fact that the underlying motional processes, being responsible for spin relaxation in both phases, are quite different. For the simulated spectra of the low-temperature phase (Figure 6) two-site jump processes between equally or unequally populated sites have been used. Here, the latter process is given by a fixed jump angle of 90° which reflects the angle separation between adjacent minima in the potential energy curve against rotation of the alkane.[6] The spectra of the high-temperature phase (Figure 7) were simulated with a six-site jump process ($2\pi/6$ jumps) between equally populated sites. Again, the simulations were done assuming a methylene segment in the pure *trans* conformational

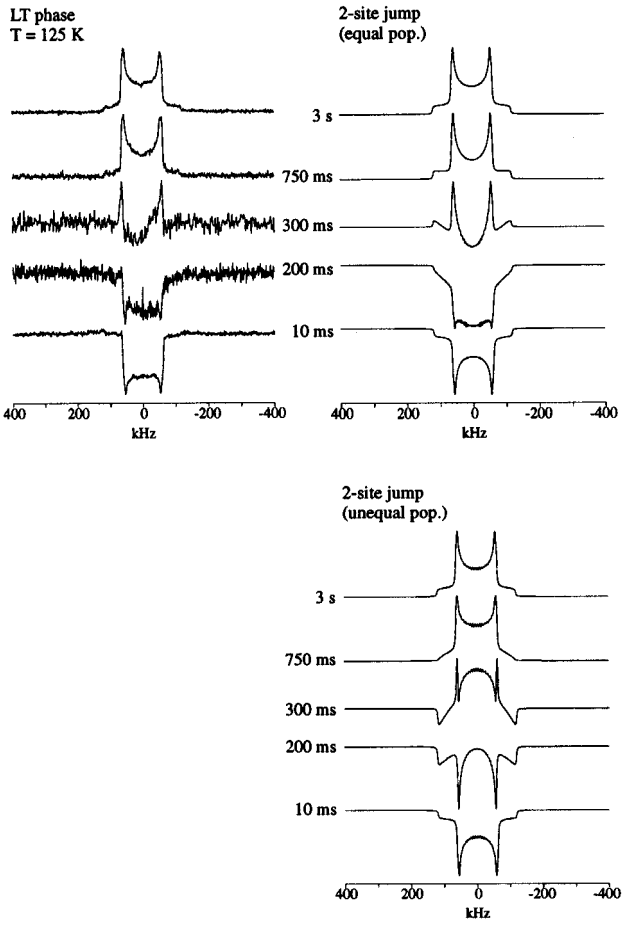

Figure 6. Partially relaxed ^{2}H NMR spectra (inversion recovery experiment) recorded for **C16−8** in the low-temperature phase (LT). For the simulation of the spectra correlation times $\tau = 8.3 \times 10^{-8}$ s (equal population, jump angle $\Delta\psi_1 = 21.5°$) and $\tau = 6.0 \times 10^{-8}$ s (unequal population, jump angle $\Delta\psi_1 = 90°$, population $p_1 = 0.97$) have been used. The relative intensities of the various spectra are given by 1.0, 0.50, 0.17, 0.23, 0.76 (experiment); 1.0, 0.70, 0.17, 0.16, 0.94 (theory, equal population); and 1.0, 0.65, 0.19, 0.23, 1.0 (theory, unequal population).

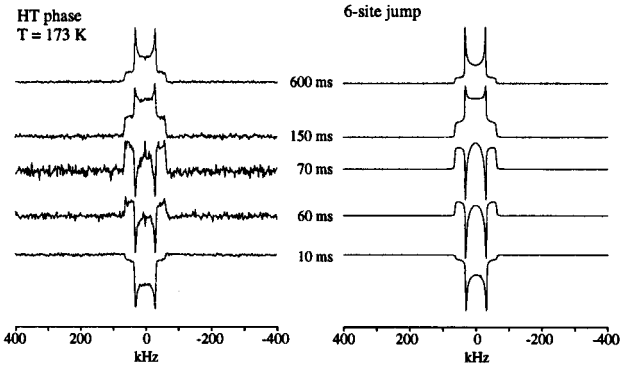

Figure 7. Partially relaxed ^{2}H NMR spectra (inversion recovery experiment) recorded for **C16−8** in the high-temperature phase (HT). For the simulation of the spectra correlation times of $\tau = 2.25 \times 10^{-11}$ s have been used. The relative intensities of the various spectra (top to bottom) are given by 1.0, 0.43, 0.19, 0.28, 0.77 (experiment) and 1.0, 0.40, 0.22, 0.30, 0.88 (theory).

state ($p_t = 1.0$) along with highly ordered chains; i.e., wobble motions perpendicular to the chain long axis are absent.

The two sets of theoretical spectra in Figure 6 demonstrate that two-site jump processes between equally and unequally populated sites can be distinguished by their T_{1Z} anisotropies. Thus, the comparison of the experimental spectra and those

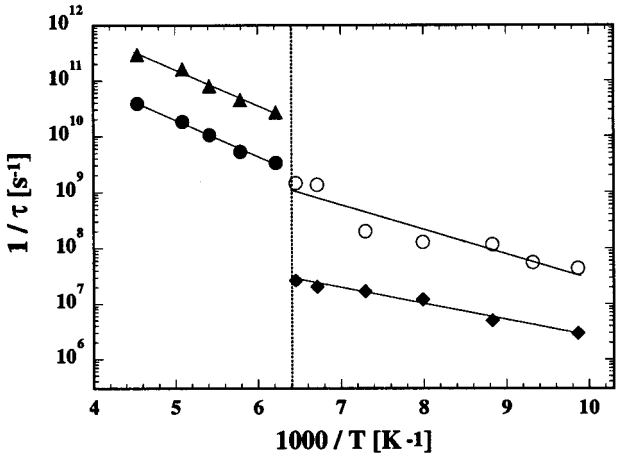

Figure 8. Arrhenius representation of the correlation times describing the molecular motions of hexadecane in urea. Low-temperature phase: two-site jump (◆), methyl group rotation (○); high-temperature phase: rotational diffusion (●), six-site jump (▲). The phase transition is indicated by the dashed line.

simulations, using the two-site jump model with unequally populated sites, reveals distinct differences. On the other hand, a good agreement with the experimental counterparts is achieved by the simulations based on the two-site jump model with equally populated sites. It therefore is concluded that the latter model is appropriate for the description of the hexadecane reorientation in the low-temperature UIC phase.

The good reproduction of the experimental spectra for both the low- and high-temperature phases can be taken as a direct proof that the model assumptions for the overall chain motions of the two UIC phases are correct. In a similar way, computer simulations have been performed for the other temperature points. They yielded the correlation times τ for overall chain motion over a large temperature range. In the case of a jump model (with equally populated sites) τ is related to the first-order rate constant k by

$$\frac{1}{\tau} = \frac{k}{p} \tag{1}$$

where p describes the relative population of one site. The final τ values are summarized in Figure 8. For the high-temperature phase two sets of data are given that refer to the results from the analysis with the six-site jump model and the rotational diffusion model, respectively. For the latter case, the following expression holds.

$$\frac{1}{\tau} = \left(\frac{2\pi}{N}\right)^2 6k \tag{2}$$

Here, N is the number of orientations and k is the first-order rate constant for the transition between neighboring sites.[23] It should be noted that the T_{1Z} anisotropy again cannot be used to distinguish between rotational diffusion and 6-fold jumps which is related to the tetrahedral symmetry of the alkane chains. For the present case, the angle between the C−^{2}H bond and the symmetry axis of the motion is 90°, which gives rise to the same T_{1Z} anisotropy in the extreme fast exchange limit for both motional models. From the data in Figure 8 the kinetic parameters (preexponential factor $1/\tau^0$, activation energy E_A) have been derived using the Arrhenius equation:

$$\frac{1}{\tau} = \frac{1}{\tau^0}\exp(-E_A/RT) \tag{3}$$

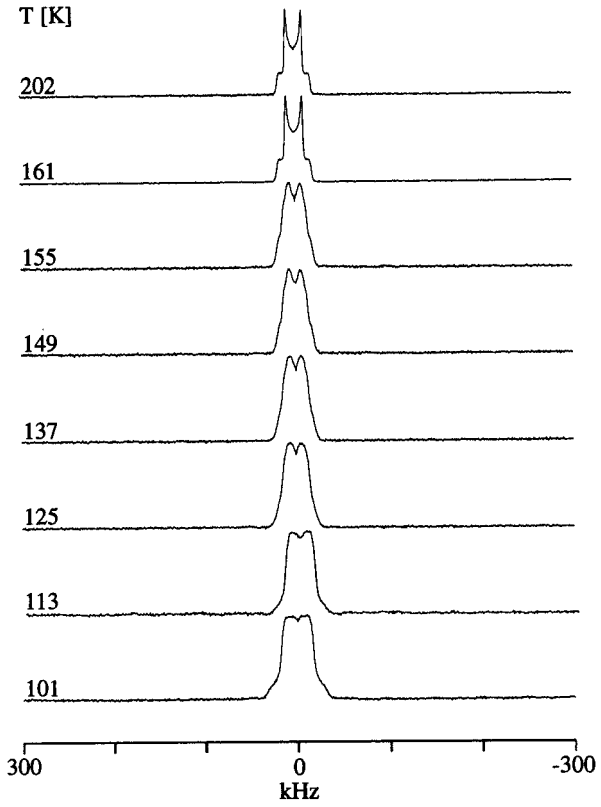

Figure 9. Variable temperature ^{2}H NMR spectra of **C16−1**.

They were found to $1/\tau^0 = 5.6 \times 10^8$ s^{-1}, $E_A = 4.0$ kJ/mol (two-site jump process, low-temperature phase), $1/\tau^0 = 2.7 \times 10^{14}$ s^{-1}, $E_A = 12.4$ kJ/mol (six-site jump process, high-temperature phase), and $1/\tau^0 = 3.6 \times 10^{13}$ s^{-1}, $E_A = 12.4$ kJ/mol (rotational diffusion, high-temperature phase).

Inspection of Figure 8 suggests that in the low-temperature phase the rate constants are in a range that they might affect the partially relaxed ^{2}H NMR spectra from quadrupole echo experiments (T_2 anisotropy). Model simulations have shown that the T_2 anisotropy is not very sensitive due to the rather small jump angles in the low-temperature phase. In addition, the rate constants are close to the fast exchange limit where line shape effects and T_2 relaxation generally lose their sensitivity for extracting dynamic processes.

In the next step, we have examined sample **C16−1**, which is deuterated at the terminal methyl group in a quite similar manner as outlined above for sample **C16−8**. Figure 9 exhibits representative experimental ^{2}H NMR spectra recorded for sample **C16−1** in the low- and high-temperature phase. The experimental ^{2}H NMR spectra are significantly narrower than those of sample **C16−8** which can be attributed to the presence of fast methyl group rotation. Line shape simulations have been done in order to reproduce the experimental spectra of sample **C16−1**. For these calculations a fast methyl group rotation has been assumed along with restricted or unrestricted overall chain rotation to describe the low- or high-temperature phase, respectively (see above). The model simulations have shown that the additional methyl group rotation presents a major contribution for the observed reduction in spectral width (reduction factor $-^1/_3$). However, there still remains a difference between the experimental and theoretical splittings of the ^{2}H NMR line shapes which suggests further motional contributions. In addition, the experimental spectra at temperatures $T < 120$ K are smeared out or broadened which cannot be reproduced by a simple superposition of various motional contributions in the fast exchange limit.

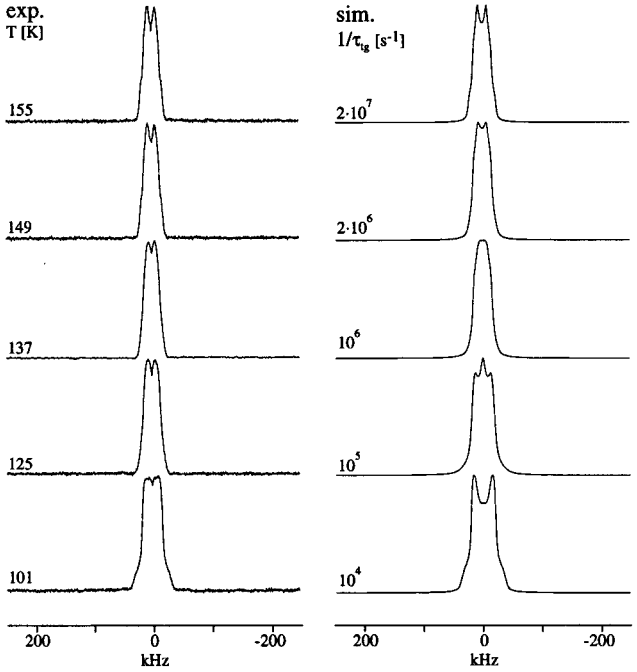

Figure 10. Experimental (left) and simulated (right) spectra of **C16−1** in the low-temperature phase. Simulations were performed assuming a two-site jump motion of the alkyl chain ($\Delta\psi_1 = 39°$, $\tau = 3.7 \times 10^{-8}$ s), methyl group rotation ($\tau < 10^{-9}$ s), and *trans−gauche* isomerization ($p_t = 0.7$) at the rates given in the figure.

The general discrepancy between the experimental and theoretical splittings for the spectra above 120 K can be overcome by the consideration of *trans−gauche* isomerizations which are very common for aliphatic chains. Figure 10 presents a series of theoretical quadrupole echo line shapes that have been obtained by the simultaneous consideration of (i) *trans−gauche* isomerization of the C2−C3 bond at various rates using a three-site model (g^+-t-g^- isomerization with $p_t = 1 - (p_{g^+} + p_{g^-})$, $p_{g^+} = p_{g^-}$ and p_i being the population of conformer i),[45,46] (ii) fast methyl group rotation, and (iii) fast overall chain rotation. These spectra refer to the low-temperature phase; i.e., the overall chain motion is modeled by a two-site jump process. The amount of *trans* conformers was kept at $p_t = 0.7$, which was found to be appropriate for a good theoretical reproduction of the experimental ^{2}H NMR spectra in the low-temperature phase. Inspection of Figure 10 reveals that the spectra between 125 and 155 K can be well described by the assumption of additional *trans−gauche* isomerizations in the fast exchange limit. The model is not appropriate, however, to describe the broadened spectral features at very low temperatures. Here, most probably a static distribution of nonequivalent methyl groups, i.e., methyl groups that experience a different chemical environment, have to be discussed.

The corresponding axially symmetric ^{2}H NMR spectra of sample **C16−1** in the high-temperature phase again can be described by taking into account methyl group rotation, *trans−gauche* isomerization, and overall chain rotation (6-fold jumps between equally populated sites). Surprisingly, the experimental splittings now give rise to a higher amount of *trans* conformers in the high-temperature phase. Just above the phase transition the *trans* content is found to $p_t = 0.95$, which remains nearly constant in the high-temperature phase. In fact, only a slight decrease to $p_t = 0.91$ at 290 K is registered.

Figures 11−13 summarize the results which were obtained from the T_{1Z} measurements of sample **C16−1**. Again, the T_{1Z}

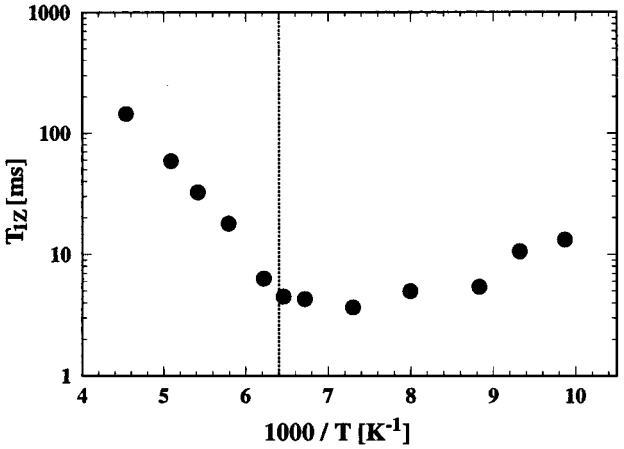

Figure 11. Experimental T_{1Z} relaxation data of **C16−1**. The dashed line indicates the phase transition.

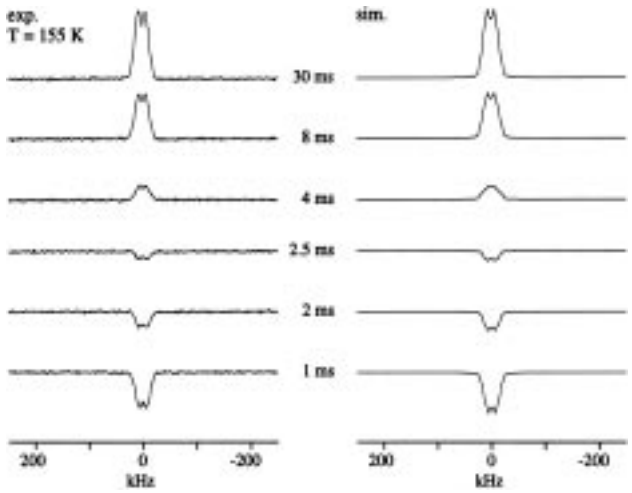

Figure 12. Experimental partially relaxed ^{2}H NMR spectra (inversion recovery experiment) recorded for **C16−1** in the low-temperature phase. The simulations (right column) have been done with the assumption of (i) a two-site jump ($\tau = 3.7 \times 10^{-8}$ s, jump angle $\Delta\psi_1 = 39°$), (ii) methyl group rotation ($\tau = 7 \times 10^{-10}$ s), and (iii) *trans−gauche* isomerization ($\tau = 10^{-8}$ s, $p_t = 0.7$).

curve in Figure 11 can be separated into two regions that are distinguished by their T_{1Z} anisotropy (see below) and that is in line with the low- and the high-temperature phase. The low-temperature part also exhibits a T_{1Z} minimum at about $T = 142$ K. It is interesting to note that the high-temperature branch above the phase transition runs parallel with the T_{1Z} curve of sample **C16−8**, discussed before. The T_{1Z} values of **C16−1**, however, generally are smaller than those of sample **C16−8**, with a factor between about 10 and 100. The largest difference is registered for the low-temperature phase where the experimental T_{1Z} values indicate the presence of a very efficient relaxation process for sample **C16−1**.

Model simulations have shown that in the low-temperature phase the underlying relaxation process can be attributed to the internal methyl group rotation. Again, this intramolecular motion might be described by either a 3-fold-jump process or by rotational diffusion that is distinguishable by partially relaxed spectra.[38,41−44] Due to the broad ^{2}H NMR spectra for the present case a final assignment of the underlying mechanism, however, is not possible. The theoretical spectra, given in Figure 12, have been obtained using a 3-fold jump process for methyl group rotation which is in agreement with the studies on other systems bearing rotating methyl groups. In a similar way the T_{1Z} data and partially relaxed spectra for the other temperature points

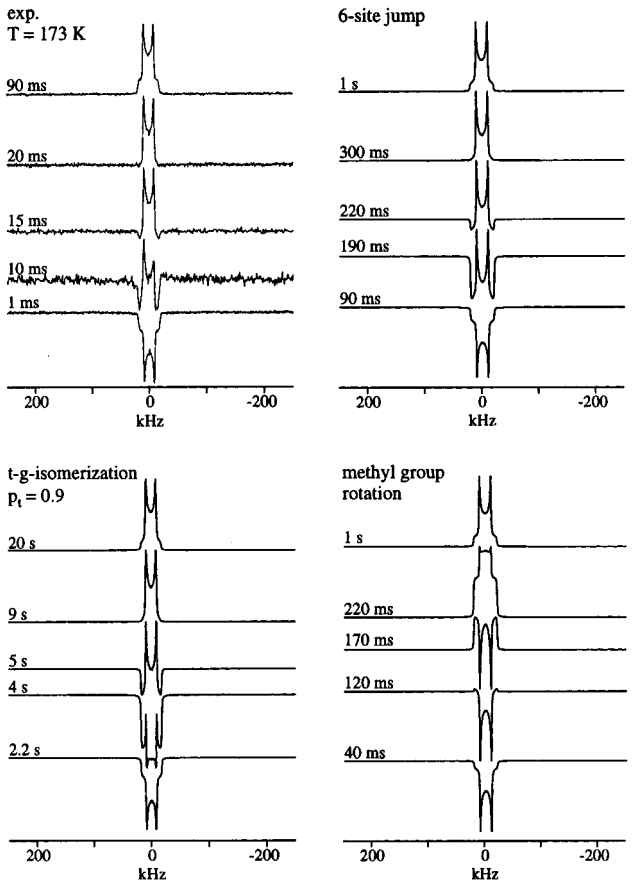

Figure 13. Partially relaxed ^{2}H NMR spectra (inversion recovery experiment) for **C16−1** in the high-temperature phase (upper left). The theoretical spectra refer to the hexadecane methyl group in the high-temperature phase with one dominant motion for spin relaxation: (i) six-site jumps (chain rotation; upper right), (ii) *trans−gauche* isomerization ($p_t = 0.9$, lower left), and (iii) methyl group rotation (lower right). The correlation times τ are 5×10^{-11} s. The spectra are plotted to the same height to demonstrate the difference in T_{1Z} anisotropy.

have been analyzed. They provided the correlation times shown in Figure 8, from which the kinetic parameters—given by $1/\tau^0 = 6.7 \times 10^{11}$ s^{-1} and $E_A = 8.4$ kJ/mol—have been derived.

The T_{1Z} relaxation in the high-temperature phase is dominated by a different motional process. This can be taken directly from the change of the slope of the T_{1Z} curve and from the partially relaxed ^{2}H NMR spectra (inversion recovery experiment, see Figure 13), which again exhibit a very characteristic T_{1Z} anisotropy. Model simulations have been performed to emphasize the influence of the three motional contributions—methyl group rotation, *trans−gauche* isomerization, and unrestricted overall chain rotation. Representative spectra from these calculations are displayed in Figure 13. Each column refers to a series of partially relaxed spectra accounting for one dominant motion responsible for spin−lattice relaxation. It is quite obvious that the T_{1Z} anisotropy and the overall T_{1Z} values strongly depend on the nature of the motional process. The comparison of such theoretical spectra with the experimental counterparts have shown that the spin−lattice relaxation in the high-temperature phase is dominated by chain rotation. In fact, the observed temperature dependence of the T_{1Z} data points to the same direction. In the high-temperature phase the slopes of the T_{1Z} curves for **C16−1** and **C16−8** are almost identical, which implies a similar motional process responsible for spin relaxation of both samples.

Simulations have been done using the rate constants for chain rotation which were obtained from the analysis of **C16−8**. The

corresponding values for methyl group rotation were taken from the extrapolation of the Arrhenius plot in Figure 8. The contribution from *trans*−*gauche* isomerization is of minor importance due to the high amount of *trans* conformers. Although the simulations could successfully reproduce the experimental T_{1Z} anisotropy, we are left with a constant difference between the experimental and theoretical overall T_{1Z} values in the high-temperature phase. That is, the theoretical T_{1Z} data are found to be larger than the experimental ones. For example at 173 K the theoretical value is given by 26 ms while the experimental value is found to 18 ms. The remaining difference might be related to further motional contributions which so far has not been accounted for.

Discussion

In the following we will discuss the experimental results from the present variable temperature ^{2}H NMR studies on UICs in conjunction with the available literature on this subject. It has been shown in the previous chapter that dynamic ^{2}H NMR spectroscopy is very suitable to obtain reliable information about the molecular features of *n*-alkane guests embedded in urea channels. A proper analysis of the corresponding line shape studies and relaxation experiments could provide a detailed picture about both the guest dynamics and their ordering behavior in such inclusion compounds. The main emphasis of the present investigation concerns the behavior of the guest species in the low-temperature phase and in the vicinity of a solid−solid phase transition upon which so far only limited information is available. In the past, UICs with *n*-alkanes or functionalized *n*-alkanes have been examined employing various experimental methods. Among these, X-ray studies,[5−10] Raman, IR,[15,16,47−51] and NMR,[11−14,26,30,52−54] spectroscopy as well as inelastic neutron scattering[55,56] have turned out to be the most suitable techniques. The majority of these studies dealt with the behavior in the high-temperature phase while studies about the molecular characteristics in the low-temperature phase are rather limited. In addition, theoretical papers[17−19] exist which focus on the solid−solid phase transitions in *n*-alkane/UICs and their impact on the molecular features of the guest components.

The following discussion of the properties of the guest species will be done primarily on a very local basis which directly is related to the local nature of the NMR technique. Details about the general structural properties of these systems, such as superstructures, etc., which have been evaluated from scattering techniques, can be found elsewhere.[3,7−10] In this connection, it should be mentioned that the hexadecane system is unique in the sense that the length of the *all-trans* chains (c = 22.8 Å) fits approximately with the doubled period of the urea framework ($2c_0$ = 22.03 Å). For this reason the UIC with hexadecane frequently has been discussed with respect to commensurate or incommensurate behavior of such systems.[3,57]

Hexadecane Dynamics. For the description of the chain dynamics in the UICs various motional contributions might be considered: (i) chain rotation, (ii) wobble motion of the chain, (iii) chain diffusion, (iv) internal *trans*−*gauche* isomerization, and (v) methyl group rotation. Among these, chain rotation, *trans*−*gauche* isomerization, and methyl group rotation have shown to play a dominant role for deuteron spin relaxation during the present study.

It has been outlined in the previous chapter that the chain dynamics is very different for the low- and high-temperature phase. This particularly is true for the overall chain (rotational) motion which in the high-temperature phase is found to possess an almost unrestricted nature. The low-temperature phase, however, is still far from the situation of complete rigid hexadecane chains. Our present NMR data analysis revealed that close to the phase transition fast, but highly restricted overall chain motions can be detected. They can be modeled by a two-site jump process of variable angle which varies with temperature between 14.5° at 103 K and 39.0° at 155 K. To some extent this behavior can be rationalized on the basis of former potential energy calculations by Chatani et al.[6] In that work the authors have shown that in the low-temperature phase the potential energy curve against the rotation of the hexadecane chain exhibits four distinct minima. They are separated by an angle of 90° and barriers up to 30 kJ/mol which prevent the chains from jumping between adjacent minima. The fact that the reorientational angle increases with temperature is in line with the observation that the distortion of the hexagonal channels decreases with increasing temperature.[6] Thus, at higher temperature the hexadecane chains experience a larger spatial freedom being consistent with an increase of the jump angle. The theoretical potential curves furthermore exhibit two distinct broad minima that are of lower energy and that would allow some oscillatory motions of the chains about their equilibrium positions. This process, which in the present work has been modeled by a simple two-site jump model, is thermally activated with an activation energy of 4 kJ/mol.

A similar model for alkane chain motion has been proposed in earlier ^{1}H NMR studies on UICs with guests such as *n*-decane, *n*-dodecane, or *n*-hexadecane[12] as well as on pure *n*-hydrocarbons.[58] In fact, during the ^{1}H NMR study on UICs[12] this "oscillatory" model was used to analyze experimental proton T_{1Z} data. In the same work it was concluded that a better description for the guest motion can be achieved by the assumption of molecular reorientation of the alkane chains between two potential minima of unequal depth. The derived (experimental) activation energy for this latter process of about 12 kJ/mol was found to be in good agreement with the potential barrier height calculated by Parsonage and Pemberton.[17] However, it should be noted that the theoretical value has been derived on the basis of the structure of the high-temperature UIC phase,[5] as expressed by the six minima in the potential energy curve. In a similar way the analysis of the proton T_{1Z} data did not distinguish between the low- and high-temperature phase. In fact, the UIC structure of the low-temperature phase was solved only recently by several X-ray investigations.[6,7,10]

In a quite similar way we have set up our two-site jump model with inequivalent sites for the low-temperature UIC phase. Here, we have considered a reorientation angle of 90°, as taken from the potential energy curve,[6] and varied the relative populations of both sites. Although the experimental biaxial line shapes (from quadrupole echo experiments) can be simulated with relative populations of the major site between 0.97 and 0.89, the "inequivalent site jump" model fails in reproducing the partially relaxed spectra from the T_{1Z} relaxation experiments (see Figure 6). This implies that a two-site jump process between unequally populated sites, i.e., adjacent minima of the energy potential curve, is not appropriate to describe the hexadecane chain overall motion in the low-temperature phase. Rather, the chains undergo oscillatory motions (two-site jumps between equivalent sites) within a deep potential well, as mentioned earlier.

Further quantitative data about the overall chain mobility in the low-temperature phase of UICs are rare. In other studies on UICs the chain mobility in the low-temperature phase is discussed on a qualitative basis. From a ^{2}H NMR investigation on perdeuterated nonadecane in urea it has been estimated that

the chains undergo rapid 30° jumps about their long axes.[13] Likewise, there was evidence for some chain mobility in the microsecond range from ^{2}H NMR studies on perdeuterated hexadecane[14] and selectively deuterated nonadecane (single-crystal study[30]) in urea. To our knowledge there exists only one further study, a quasielastic neutron scattering (IQNS) investigation,[56] where the low-temperature dynamics has been described quantitatively. The experimental analysis with a combined rotational−translational model has shown that the IQNS data are consistent with a restricted overall rotation in the low-temperature phase and a jump angle of 28° at 160 K. However, the time scale is much different from that evaluated during the present NMR work. Thus, from the IQNS study the overall motion was found to be in the order of 10^{11} s^{-1} while our NMR data analysis yields chain rotations in the order of 10^7 s^{-1}. So far, the reason for this discrepancy of the absolute rates is unknown. It seems to be rather unlikely that the difference in overall chain motion is due to the different chain lengths. One reason might be found in the different model approaches used for the data analysis during the present NMR work and during the earlier IQNS study. On the other hand, it should be kept in mind that the experimental T_{1Z} data (see Figure 5) unequivocally show that the chain rotation must occur on a time scale being slower than the Larmor frequency ($k < 10^9$ s^{-1}).

The nature of the overall motion (type and time scale) changes completely if the temperature is raised above the phase transition. Now, the chains are able to rotate almost unhindered about their long axes which might be described either by rotational diffusion or 6-fold jumps. In addition, the rates of the overall rotation are found to be in the order of 10^{10} s^{-1}; i.e., they have increased at the phase transition by about 3 orders of magnitude. According to theoretical calculations,[6] the potential energy curve of the high-temperature curve displays six potential minima with barrier heights of about 6 kJ/mol. The hexadecane chains thus can easily jump into neighboring sites. It is therefore very likely that rather a 6-fold jump process than rotational diffusion is the appropriate model for overall chain motion in the high-temperature phase. As mentioned earlier, the present NMR data cannot provide an unequivocal proof for the correct motional model which is related to the special geometry of the alkane chains. The activation energy for overall rotation in the high-temperature phase is found to 12.4 kJ/mol, which is about twice the barrier height derived from the potential energy calculations.[6]

It has been mentioned that various studies exist dealing with the high-temperature phase behavior of UICs. Again, we refer to the IQNS study[56] on nonadecane/urea from which overall chain rotations (6-fold jumps) in the order of 10^{11} s^{-1} and an activation energy of 2.2 kJ/mol have been derived. In a further Raman investigation an activation energy of 4.8 kJ/mol for overall chain rotation has been reported.[15] Furthermore, there exists a single-crystal ^{2}H NMR study on nonadecane/urea[26] where the authors contrast various motional models to account for the spin relaxation in the high-temperature phase. The overall chain rotation—which has been modeled by a diffusive process—again is on a similar time scale (10^{11} s^{-1}), while the activation energy was found in the order of about 9 kJ/mol, slightly depending on the actual simulation parameters. Obviously, there exists a discrepancy between the activation energies evaluated from the ^{2}H NMR and the IQNS or Raman studies which is not yet understood. One reason could be related to the different motional models used during the various studies. A complementary study performed on the same system comprising various experimental techniques certainly would be very helpful to overcome this problem.

From the previously discussed single-crystal ^{2}H NMR work on nonadecane/urea[26] there is evidence that between 260 and 333 K the alkane chains undergo a significant wobble motion of the chain long axes with an opening angle between 20° and 30°. The rate constants are found to be slower by a factor of 5−10 than the overall chain rotation about the long axis while the activation energy again is about 9 kJ/mol. From the present analysis, we have concluded that a similar wobble motion does not exist for the hexadecane chains below 290 K. This has been taken directly from the experimental splittings of sample **C16−8** which remain almost constant throughout the whole high-temperature phase up to 290 K. One might speculate whether the missing wobble motion is related to the different chain lengths of hexa- and nonadecane. However, it should be recalled that different quadrupolar coupling constants have been used in the present NMR work and during the earlier single-crystal NMR study. While we have taken a value of 167 kHz, in the former study quadrupolar coupling constants above 186 kHz have been used. Such values appear to be unusually high for aliphatic deuterons. Another reason for the different results for the nona- and hexadecane chains might be found in the consideration of the conformational order. This contribution was not considered explicitly during the earlier analysis of the UIC with nonadecane. On the other hand, there is clear evidence from several spectroscopic investigations that the conformational disorder is of importance in such systems which holds in particular for the low-temperature phase (see below).

Apart from the overall chain motions, two types of internal motions—*trans*−*gauche* isomerizations of the C2−C3 bond and methyl group rotation—have been established by the present NMR analysis. Line shape simulations using a three-site jump model (g^+-t-g^-)[45,46] for chain isomerization have shown that in the low-temperature phase this process occurs with rate constants being $\geq 10^7$ s^{-1}, i.e., on the fast NMR time scale. An exact determination of the corresponding rates was not possible, since—as will be shown below—the T_{1Z} relaxation is dominated by the methyl group rotation. It should be noted that the ^{2}H NMR measurements performed on UICs with *n*-alkanes of length $n = 15$, 19, 20 bearing deuterated methyl groups have shown similar results for the conformational dynamics.[59] Obviously, *n*-alkanes in urea possess a high degree of conformational flexibility which can be transferred also to the low-temperature phase. In this respect, they resemble phospholipid chains[20,21] in the liquid crystalline phase or melts from polymers with aliphatic chain components[22,23] which also exhibit a high internal flexibility in terms of fast *trans*−*gauche* isomerization. In the high-temperature range the time scale of the *trans*−*gauche* isomerization again could not be quantified via T_{1Z} measurements since this internal process is obscured by other motional contributions. From the available experimental data there is no doubt that *trans*−*gauche* isomerization appears on a very fast time scale. Further information about this process is expected from a forthcoming study of *n*-alkane chains that are selectively deuterated at the C2 or C3 methylene group.

The second internal motion is given by the rotation of the methyl group. This process was found to dominate the T_{1Z} relaxation of sample **C16−1** in the low-temperature phase with rate constants in the order of 10^9-10^{10} s^{-1}. The activation energy of 8.4 kJ/mol, derived for this process, is within the range reported from other studies on methyl group rotation.[60−65] In the high-temperature phase the methyl group motion could not be determined since the T_{1Z} relaxation of compound **C16−1** is

found to be dominated by the overall chain rotation. It therefore is still open whether this motion is affected by the solid−solid phase transition. Again, absolute values for methyl group rotations of alkanes trapped in UIC are rare. A former analysis of IR band shapes performed for various UICs revealed rate constants in the order of 10^{12} s^{-1} and activation energies between 12.5 an 14.7 kJ/mol also for the high-temperature phase.[47] Likewise, the earlier mentioned ^{2}H NMR study on the UIC with nonadecane[26] has shown that in the high temperature the methyl group rotation occurs on a similar time scale. The activation energy has been estimated to be between 8.5 and 10 kJ/mol. Here, an additional wobble motion of the methyl group also has been introduced for the analysis of the experimental T_{1Z} data.

Studies on other systems bearing methyl groups have shown that in the solid state the kinetic parameters strongly depend on the particular system. For example, in L-alanine the crystal packing gives rise to a significant slowdown of the methyl group rotation.[62,64] As a result, the rate constants for methyl group rotation are about 3 orders of magnitude smaller than those reported for other systems such as methyl *p*-nitrobenzenesulfonate with less hindered methyl groups.[65] The observed rate constants obtained for the UIC with hexadecane suggest that again we have to deal with less hindered methyl groups. The same conclusion can be drawn from the evaluated activation energy. The value of 8.4 kJ/mol is close to the values reported for other aliphatic methyl groups. It should be mentioned that ^{2}H NMR experiments have been performed for UICs with other *n*-alkanes (n = 15, 19, 20), deuterated at the terminal methyl groups. These data suggest that in the low-temperature phase the methyl group rotation can be regarded as the dominant T_{1Z} relaxation mechanism for such inclusion compounds.[59]

Translational motions of the guest species within the urea channels represent a further important motional process in these systems. Such motions have been characterized by IQNS experiments.[56] It was reported that for the UIC with nonadecane these motions show up on the picosecond time scale in the high-temperature phase, while they are absent in the low-temperature phase. Recent molecular dynamic simulations came up with similar conclusions.[66] We certainly cannot get direct information about such translational motions from the present ^{2}H NMR experiments. However, it is assumed that indirectly such motions give rise to the changes of the residual $1/\pi T_2^0$ values of the experimental NMR line shapes. Thus, in the low-temperature phase a value of $1/\pi T_2^0 = 3$ kHz has been used for the line shape fitting while for the high-temperature phase a value of 1 kHz was found to be sufficient. The residual $1/\pi T_2^0$ value contains those magnetic interactions that otherwise were not considered explicitly. For the present case, $1/\pi T_2^0$ should contain contributions from homonuclear (^{2}H−^{2}H) and heteronuclear (^{2}H−^{1}H) dipolar interactions. The latter part could be further subdivided into intra- and intermolecular contributions. The reduction in residual $1/\pi T_2^0$ at the phase transition is attributed to the loss of the intermolecular contribution between the guest molecules and the rigid urea matrix. That is, in the high-temperature phase the fast rotational and translational motions result in an averaging of the intermolecular dipolar interactions. Similar observations have been reported for deuterated six-membered rings in cyclophosphazene inclusion compounds.[67]

At present, we are left with the result that the T_{1Z} data of sample **C16−1** in the high-temperature phase cannot be completely described on the basis of the proposed motional model with contributions from chain rotation, *trans*−*gauche* isomerization, and methyl group rotation. The calculated T_{1Z} values thus are constantly larger than the experimental ones. To overcome this problem, one might increase the quadrupolar coupling constant of the methyl group which, however, appears to be somehow arbitrary. On the other hand, it might be possible that other motional contributions, such as additional wobble motions near the chain ends, have to be taken into account. Forthcoming studies on samples with hexadecane chains deuterated at other positions along the chain (C2, C3, etc.) should give further information about such additional motional contributions.

Molecular Order. The discussion of the alkane chain order again requires the consideration of three contributions: (i) conformational order, (ii) orientational order, and (iii) positional order. While the present ^{2}H NMR investigations allow a determination of the contributions from conformational and orientational order, they are not appropriate to provide information about the positional order.

The orientational order can be described by considering the alignment of the alkane chain long axes with respect to the urea channel axis (*c*-axis) and the horizontal distribution of the alkane chains about the channel axis. The analysis of the ^{2}H NMR data has shown that the alkane chains (long axis) are perfectly aligned with respect to the urea channel which holds for both the high- and low-temperature phase. The horizontal orientation of the hexadecane chains behaves differently. In the low-temperature phase, there exists a preferential orientation that is evident from X-ray investigations and the potential energy calculations,[6,17] as discussed earlier. At elevated temperatures the hexadecane chains start to undergo restricted rotational motions, described by a 2-fold jump process. This process is accompanied by a loss of orientational order which gives rise to a small amount of dynamic disorder. Upon heating above the phase transition, the restricted chain rotation is replaced by an almost unhindered rotation of the chains about their long axes. As a result, we have to deal with a random horizontal distribution of the hexadecane chains, i.e., a large degree of dynamic disorder. This suggests that the phase transition can be assigned to a dynamic order−disorder transition. Other studies on UICs employing IR, Raman,[15,16,47−51] IQNS,[55,56] and NMR[13,14,26,30,52−54] techniques have demonstrated that the latter dynamic disorder can be regarded as a general phenomenon encountered in the high-temperature phase of such systems. It should be mentioned that our result of a perfect alignment of the alkane chains differs from a previous single-crystal ^{2}H NMR work on the UIC with nonadecane.[26] In that study the authors discussed a chain wobble motion which gives rise to a significant reduction in longitudinal chain order. This discrepancy might be related to the higher quadrupole coupling constant used in that work, being larger than typical static values. We have used for the present analysis the static value which has been derived from the low-temperature spectrum and which is claimed to be a reasonable way of analysis. In this connection, it is expected that forthcoming studies at cryogenic temperatures could help to solve the problem of the correct quadrupolar coupling constant in such systems.

Former X-ray investigations[5−10] on UICs with *n*-alkanes have shown that the guest molecules possess a high degree of positional order in the low-temperature phase. IQNS experiments have demonstrated that in the high-temperature phase due to translational motions the positional order is reduced.[56] As a result, one has to deal with a further contribution to the dynamic disorder for such UIC systems.

In the following, we discuss the results for the conformational

order in connection with the available data on similar UICs. The variable temperature ^{2}H NMR investigations of the present work have shown that the central part of the hexadecane chains (C8−C9) can be regarded as a segment that exists exclusively in the *trans* conformational state throughout the whole temperature range examined here. At the same time, the chain ends (C2−C3 bond) possess some conformational flexibility that is expressed by a *trans* content less than unity. Thus, in the low-temperature phase the data analysis yields a *trans* content of $p_t = 0.7$, which surprisingly increases ($p_t = 0.95$) upon heating above the phase transition.

Various studies—including Raman, IR,[15,16,47−51] and NMR[13,14,26,30,52−54] studies as well as molecular mechanics[52] and dynamics[66,68,69]—exist that deal with the conformational behavior of the alkane chains in the UIC high-temperature phase and that gave rise to some dispute about the "true" conformational order in terms of *trans* and *gauche* conformers. There is no doubt that the inner parts adopt the *all-trans* conformation. The reported content of *trans* conformers for the C2−C3 bond, however, varies between $p_t = 0.77$ and 0.97, depending on the particular experimental technique. The lowest values were derived from a combined switched angle spinning ^{13}C NMR and molecular mechanics study[52] which came up with p_t values between 0.77 and 0.82, depending on the particular alkane chain length. Higher values with $p_t \geq 0.9$ have been reported from ^{2}H NMR studies,[30,32] while the upper limit of 0.95−0.97 is given by IR and Raman studies[15,16,47−51] as well as molecular dynamics studies.[66] Again, our values for the high-temperature phase are in agreement with a recent ^{2}H NMR study on nonadecane in urea[30,32] and close to those given from IR and Raman studies.[15,16,47−51]

A comparison of the present conformational data for the low-temperature phase is difficult. To our knowledge there exists only a Raman study[16] from which a value of $p_t \geq 0.92$ has been estimated. This value is much higher than that derived from the present ^{2}H NMR investigations. It should be mentioned that preliminary experiments on UICs with other chain lengths ($n = 15, 19, 20$) reveal a similar decrease of the amount of *trans* conformers upon cooling to the low-temperature phase. In addition, there are indications that the length of the alkane chain also has some influence on the actual *trans* content within the low-temperature phase.[59] At first sight, it seems to be surprising that the content of *trans* conformers is reduced in the low-temperature phase. These findings might be rationalized by the specific arrangement of the guests due to the distorted hexagonal symmetry of the urea channels. Thus, the hexadecane chains exhibit the same horizontal orientation within one urea channel and are able to undergo only some restricted rotational motions. At the same time, the alkane chains have to move together due to the shrinkage of the urea channel along the *c*-direction.[6] Since the chain ends on average are oriented in the same horizontal direction, the *all-trans* chain conformation now is energetically less favored. Hence, the alkane chains try to avoid this situation on the expense of increasing *gauche* conformers at the chain ends. This assumption is supported by ^{2}H NMR measurements on the UIC with pentadecane. Here, a higher amount of *trans* conformers is found in the low-temperature phase than for hexadecane, which is in line with the reported expansion of the urea lattice along the *c*-direction.[70] The observation of changes in conformational order at the solid−solid phase transition is not restricted to the present ^{2}H NMR studies. Rather, recent variable temperature ^{13}C MAS NMR investigations on UICs with *n*-alkanes of different lengths have revealed distinct changes in the ^{13}C NMR spectra which again reflect an impact on the conformational order by the solid−solid phase transition.[59]

A recent study[19] of the dependence of the solid−solid phase transition on the alkane chain length came to the conclusion that the low- and high-temperature phases are distinguished by the conformational order of the alkane chains. In the low-temperature phase the alkane chains are assumed to adopt the *all-trans* conformation while conformational defects are present in the high-temperature phase. The authors were able to describe the dependence of the phase transition temperatures with the assumption that conformational defects only exist in the high-temperature phase. The present NMR analysis has revealed a quite different situation for the UIC with hexadecane, as expressed by a high degree of conformational disorder at the chain ends in the low-temperature phase. At the same time, the conformational disorder is substantially reduced upon heating to the high-temperature phase. These findings imply that the description of the phase transition temperatures on the basis of pure conformational defects is not sufficient. Furthermore, one should keep in mind that there exist large spatial constraints by the surrounding urea lattice. Due to sterical reasons, it is almost impossible that the alkane chains possess a conformational defect in the inner part of the chains.

We close with some comments on the broadened spectra observed for sample **C16−1** at temperatures below 120 K. At present, it is believed that these spectra stem from a static distribution of different nonequivalent molecules which most probably is due to a different content of *gauche* conformers. It should be mentioned that there are indications that the UIC with hexadecane exhibits an additional phase transition[7] at 120 K about which, so far, very little is known. It thus is very likely that there is a connection between this second phase transition and the appearance of such unusual and broadened ^{2}H NMR line shapes. This assumption of a unique property of the hexadecane/urea system is further supported by the fact that similar effects were not observed during the ^{2}H NMR experiments on other UICs with *n*-alkanes of length $n = 15, 19, 20$.[59] Forthcoming ^{2}H NMR experiments below 90 K might yield further information about the molecular reasons for this experimental observation.

Conclusions

The urea inclusion compound with *n*-hexadecane has been studied over a large temperature range by dynamic ^{2}H NMR spectroscopy. These techniques in connection with selectively deuterated guest compounds are well suitable to evaluate the structural and dynamical features of the guest species. It has been demonstrated that the quantitative analysis of the spin−lattice relaxation data are of particular help for the determination of the various motional contributions present in such systems. The data analysis has been done by describing the chain dynamics for both the high- and low-temperature phase by a superposition of three major contributions: (i) chain rotation, (ii) *trans*−*gauche* isomerization, and (iii) methyl group rotation. The most prominent result refers to the overall rotation. There is evidence that a fast but highly restricted rotational process (oscillatory motion) is dominant in the low-temperature phase. Upon heating to the high-temperature phase the overall chain motion is described by an almost unrestricted chain rotation process that gives rise to rotational disorder of the chains. The phase transition therefore has been assigned to a dynamic order−disorder transition. The internal motional contributions—*trans*−*gauche* isomerization and methyl group rotation—are found to be on the fast NMR time scale throughout the whole temperature

range covered here. The alkane chains furthermore are characterized by a flexibility gradient that is affected by the solid−solid phase transition. Thus, the inner segments are found to be in the *trans* conformational state which holds for both the low- and high-temperature phase. The outer chain segments (C2−C3 bond) possess a considerable amount of *gauche* conformers which surprisingly is lowered in the high-temperature phase. It is assumed that this phenomenon is related to the sterical hindrance of the chains in the urea channels. In summary, the present ^{2}H NMR study has provided new details about the molecular features of *n*-alkane chains in UICs in the low- and high-temperature phase. Studies on other UIC samples with selectively deuterated alkanes of different lengths are in progress which should provide information about the influence of the particular chain length (odd−even effect) on the molecular parameters.

Appendix

In the following we briefly review the theoretical background for the simulations of dynamic ^{2}H NMR experiments including quadrupole echo line shapes, relaxation data, and partially relaxed spectra. As outlined elsewhere (see for example refs 20−24, 41, 43, 71, and 72), the free induction decay starting at the top of the quadrupole echo is given by

$$S(t,\tau_1,\tau_2) = \mathbf{1}\exp(\mathbf{A}t)\exp(\mathbf{A}\tau_2)\exp(\mathbf{A}\tau_1)^*\boldsymbol{\sigma}(0) \quad \text{(A1)}$$

The derivation of eq A1 assumes infinitesimal short radio-frequency pulses (δ-pulses). $\sigma(0)$ refers to transverse magnetization at the beginning of the experiment and is given by the fractional population of the *N* exchanging sites. **A** is a complex matrix of size *N* which can be subdivided into two parts (see eq A2).

$$\mathbf{A} = \mathrm{i}\boldsymbol{\Omega} + \mathbf{K} \quad \text{(A2)}$$

The imaginary part of **A** is given by the diagonal matrix $\boldsymbol{\Omega}$ whose elements Ω_{ii} describe the frequencies of the exchanging sites. The real part corresponds to a kinetic matrix **K**. Here, the nondiagonal elements k_{ij} are the jump rates from site *j* to *i*, while the diagonal elements k_{ii} represent the sums of the jump rates for leaving site *i*. In addition, the k_{ii} contain the residual line widths in terms of $1/T_2^0$ which reflect contributions from homo- and heteronuclear dipolar interactions of the spin Hamiltonian. Depending on the complexity of the system studied several internal and intermolecular processes can be superimposed. Usually, cross-terms between the various processes are neglected;[73,74] i.e., the various motions are assumed to be independent from each other. For the present case of the hexadecane chains the biggest matrix has a size of $N = 54$, which reflects three sites for methyl group rotation, three sites for *trans*−*gauche* isomerization, and six sites for overall chain rotation. Further details about other motional models including jump motions and diffusive processes can be found elsewhere (see for example refs 24 and 43). Equation A1 can be solved numerically using standard diagonalization routines.[37] From this, ^{2}H NMR line shapes, partially relaxed spectra, and spin−spin relaxation times can be derived.

The simulation of partially relaxed ^{2}H NMR spectra from the modified inversion recovery experiment (see Experimental part) is feasible with the help of eq A3.[41]

$$S(t,\tau_1,\tau_2,\tau_r) = [1 - 2\exp(-\tau_r/T_{1Z})]S(t,\tau_1,\tau_2) \quad \text{(A3)}$$

τ_r refers to the variable interval between the inversion pulse and the quadrupole echo sequence used for signal detection. The spin−lattice relaxation time T_{1Z} is obtained from

$$\frac{1}{T_{1Z}} = \frac{3}{16}\left(\frac{e^2qQ}{\hbar}\right)^2[J_1(\omega) + 4J_2(2\omega)] \quad \text{(A4)}$$

e^2qQ/h is the quadrupolar coupling constant with a typical value of 170 kHz whose actual size depends on the chemical surroundings of the deuteron. As described in refs 38 and 73, the spectral densities J_m for a *N*-site problem can be derived by solving the following equation

$$J_m(\omega) = 2\sum_{a,a'=-2}^{2} d^{(2)}_{ma}(\theta')\, d^{(2)}_{ma'}(\theta') \sum_{n,l,j=1}^{N} X_l^{(0)} X_l^{(n)} X_j^{(0)} X_j^{(n)}$$
$$d^{(2)}_{0a}(\theta_l'')d^{(2)}_{0a}(\theta_j'')\cos(a\phi_l - a'\phi_j)\frac{\lambda_n}{\lambda_n^{\,2} + \omega^2};$$
$$\phi_i = \phi_i'' - \phi' \quad \text{(A5)}$$

Here, $X^{(n)}$ and λ_n are the corresponding eigenvectors and eigenvalues of the symmetrized rate matrix **K′**, the angles θ'' and ϕ'' are the polar angles between the principal axis and the intermediate axis (motional axis) system, and the angles θ' and ϕ' are those between the intermediate and the laboratory axis system, respectively. $d_{ab}^{(2)}(\theta)$ are elements of the reduced Wigner rotation matrix. If there is a superposition of several motional modes, then the transformation from the principal axis system to the laboratory frame is subdivided into several steps according to the number of motional contributions. For example, the analysis of the data for compound **C16−1** implies the presence of methyl group rotation, *trans*−*gauche* isomerization, and overall chain rotation which is in line with four transformations between the principal axis and laboratory system.

Equation A5 describes the most general case to calculate the spin−lattice relaxation time T_{1Z}. However, for a series of simple molecular processes, such as 3-fold jumps or free rotation, analytical expressions exist.[38] They easily can be implemented into the line shape program (eq A3) and also have been used during the course of the present investigations for some limiting cases.

Acknowledgment. We thank Mrs. H. Seidel for the synthesis of the selectively deuterated *n*-alkanes. Financial support by the Deutsche Forschungsgemeinschaft and the Fonds der Chemischen Industrie is gratefully acknowledged.

References and Notes

(1) Schlenk, W. *Liebigs Ann. Chem.* **1949**, *204*, 565.
(2) Atwood, J. L., Davies, J. E. D., MacNicol, D. D., Eds. *Inclusion Compounds*; Academic Press: New York, 1984; Vols. 1−3; Oxford University Press: Oxford, 1991; Vols. 4 and 5.
(3) Hollingsworth, M. D.; Harris, K. D. M. In *Comprehensive Supramolecular Chemistry*; Atwood, J. L., Davies, J. E. D., MacNicol, D. D., Voegtle, E., Eds.; Pergamon Press: 1996; Vol. 6, p 177.
(4) Pemberton, R. C.; Parsonage, N. G. *Trans. Faraday Soc.* **1965**, *61*, 2112.
(5) Smith, A. E. *Acta Crystallogr.* **1952,** *5*, 224.
(6) Chatani, Y.; Anraku, H.; Taki, Y. *Mol. Cryst. Liq. Cryst.* **1978**, *48*, 219.
(7) Forst, R.; Boysen, H.; Frey, F.; Jagodzinski, H.; Zeyen, C. *J. Phys. Chem. Solids* **1986**, *47*, 1089.
(8) Forst, R.; Jagodzinski, H.; Boysen, H.; Frey, F. *Acta Crystallogr.* **1986**, *B43*, 187.
(9) Forst, R.; Jagodzinski, H.; Boysen, H.; Frey, F. *Acta Crystallogr.* **1989**, *B46*, 70.
(10) Harris, K. D. M.; Gameson, I.; Thomas, J. M. *J. Chem. Soc., Faraday Trans.* **1990**, *86*, 3135.

(11) Gilson, D. R. F.; McDowell, C. A. *Mol. Phys.* **1961**, *4*, 125.
(12) Bell, J. D.; Richards, R. E. *Trans. Faraday Soc.* **1969**, *65*, 2529.
(13) Casal, H. L.; Cameron, D. G.; Kelusky, E. C. *J. Chem. Phys.* **1984**, *80*, 1407.
(14) Harris, K. D. M.; Jonsen, P. *Chem. Phys. Lett.* **1989,** *154*, 593.
(15) Kobayashi, M.; Koizumi, H.; Cho, Y. *J. Chem. Phys.* **1990**, *93*, 4659.
(16) Baghdadi, A. E.; Guillaume, F. *J. Raman Spectrosc.* **1995**, *26*, 155.
(17) Parsonage, N. G.; Pemberton, R. C. *Trans. Faraday Soc.* **1967**, *63*, 311.
(18) Linden-Bell, R. M. *Mol. Phys.* **1993**, *79*, 313.
(19) Fukao, K. *J. Chem. Phys.* **1990**, *92*, 6867.
(20) Griffin, R. G. *Methods Enzymol.* **1981**, *72*, 108.
(21) Davis, J. H. *Biochim. Biophys. Acta* **1983**, *737*, 117.
(22) Spiess, H. W. *Adv. Polym. Sci.* **1985**, *66*, 23.
(23) Müller, K.; Meier, P.; Kothe, G. *Prog. Nucl. Magn. Reson. Spectrosc.* **1985**, *17*, 211.
(24) Vold, R. R.; Vold, R. L. *Adv. Magn. Opt. Res.* **1991**, *16*, 85.
(25) Ripmeester, J. In *Inclusion Compounds*; Atwood, J. L., Davies, J. E. D., MacNicol, D. D., Eds.; Oxford University Press: 1991; Vol. 5, p 37.
(26) Greenfield, M. S.; Vold, R. L.; Vold, R. R. *Mol. Phys.* **1989,** *66,* 269.
(27) Meirovitch, E.; Krant, T.; Vega, S. *J. Phys. Chem.* **1983**, *87*, 1390.
(28) Poupko, R.; Furman, E.; Müller, K.; Luz, Z. *J. Chem. Phys.* **1991**, *95*, 407.
(29) Greenfield, M. S., Vold, R. L.; Vold, R. R. *J. Chem. Phys.* **1985**, *83*, 1440.
(30) Baghdadi, A. E.; Dufourc, E. J.; Guillaume, F. *J. Phys. Chem.* **1996**, *100*, 1746.
(31) Heaton, N. J.; Vold, R. L.; Vold, R. R. *J. Magn. Reson.* **1989,** *84*, 333.
(32) Cannarozzi, G. M.; Meresi, G. H.; Vold, R. L.; Vold, R. R. *J. Phys. Chem.* **1991**, *95*, 1525.
(33) Warner, R. M.; Leitch, L. C. *J. Labelled Compd.* **1965**, *1*, 42.
(34) Baer, T. A.; Carney, R. L. *Tetrahedron Lett.* **1976,** *51*, 4697.
(35) Heaton, N. J.; Vold, R. R.; Vold, R. L. *J. Magn. Reson.* **1988**, *77*, 572.
(36) Müller, K. To be published.
(37) Smith, B. T.; Boyle, J. M.; Garbow, B. S.; Ikebe, Y.; Klema, V. C.; Moler, C. B. *Matrix Eigensystem Routines-EISPACK Guide*; Springer-Verlag: Berlin, 1976.
(38) Torchia, D. A.; Szabo, A. *J. Magn. Reson.* **1982**, *42*, 107.
(39) Schmidt, C.; Blümich, B.; Spiess, H. W. *J. Magn. Reson.* **1988**, *79*, 269.
(40) Lin, T.-H.; Vold, R. R. *J. Phys. Chem.* **1991**, *95*, 9032.
(41) Wittebort, R. J.; Olejniczak, E. T.; Griffin, R. G. *J. Chem. Phys.* **1987**, *86*, 5411.
(42) Müller, K.; Wassmer, K. H.; Kothe, G. *Adv. Polym. Sci.* **1990**, *95*, 1.
(43) Vold, R. R. In *NMR Probes of Molecular Dynamics*; Tycko, R., Ed.; Kluwer Academic Publishers: Dordrecht, 1994; p 27.
(44) Tang, J.; Sterna, L.; Pines, A. *J. Magn. Reson.* **1980**, *41*, 389.
(45) Petersen, N. O.; Chan, S. I. *Biochemistry* **1977**, *16*, 2657.
(46) Edholm, O.; Blomberg, C. *Chem. Phys.* **1980**, *53*, 185.
(47) MacPhail, R. A.; Snyder, R. G.; Strauss, H. L. *J. Chem. Phys.* **1982**, *77*, 1118.
(48) Marconelli, M.; Strauss, H. L.; Snyder, R. G. *J. Chem. Phys.* **1985**, *82*, 2811.
(49) Wood, K. A.; Snyder, R. G.; Strauss, H. L. *J. Chem. Phys.* **1989**, *91*, 5255.
(50) Casal, H. *J. Phys. Chem.* **1990**, *94*, 2234.
(51) Smart, S. P.; Baghdadi, A. E.; Guillaume, F.; Harris, K. D. M. *J. Chem. Soc., Faraday Trans.* **1994**, *90*, 1313.
(52) Imashiro, F.; Kuwahara, D.; Nakai, T.; Terao, T. *J. Chem. Phys.* **1989**, *90*, 3356.
(53) Okazaki, M.; McDowell, C. A. *J. Mol. Struct.* **1984**, *118*, 149.
(54) Imashiro, F.; Maeda, T.; Nakai, T.; Saika, A.; Terao, T. *J. Phys. Chem.* **1986**, *90*, 5498.
(55) Boysen, H.; Frey, F.; Blank, H. *Mater. Sci. Forum* **1988**, *27/28*, 123.
(56) Guillaume, F.; Sourisseau, C.; Dianoux, A. J. *J. Chem. Phys.* **1990**, *93*, 3536.
(57) Rennie, A. J. O.; Harris, K. D. M. *J. Chem. Phys.* **1992**, *96*, 7117.
(58) Andrew, E. R. *J. Chem. Phys.* **1950**, *18*, 607.
(59) Schmider, J.; Müller, K. Manuscript in preparation.
(60) Takegoshi, K.; Imashiro, F.; Terao, T.; Saika, A. *J. Chem. Phys.* **1984**, *80*, 1089.
(61) Hiyama, Y.; Roy, S.; Cohen, J. S.; Torchia, D. A. *J. Am. Chem. Soc.* **1989**, *111*, 8609.
(62) Beshah, K.; Olejniczak, E. T.; Griffin, R. G. *J. Chem. Phys.* **1987**, *86*, 4730.
(63) Kintanar, A.; Alam, T. M.; Huang, W.; Schindele, D. C.; Wemmer, D. A.; Drobny, G. *J. Am. Chem. Soc.* **1988**, *110*, 6367.
(64) Schleicher, A.; Müller, K.; Kothe, G. *J. Chem. Phys.* **1990**, *92*, 6432.
(65) Hiraoki, T.; Hamada, T.; Tsutsumi, A. *J. Mol. Struct.* **1995**, *355*, 143.
(66) Souaille, M.; Guillaume, F.; Smith, J. C. *J. Chem. Phys.* **1996**, *105*, 1516, 1529.
(67) Liebelt, A.; Müller, K. Manuscript in preparation.
(68) Vold, R. L.; Vold, R. R.; Heaton, N. J. *Adv. Magn. Reson.* **1989**, *13*, 17.
(69) Lee, K.-J.; Mattice, W. L.; Snyder, R. G. *J. Chem. Phys.* **1992**, *96*, 9138.
(70) Hollingsworth, M. D. Private communication.
(71) Spiess, H. W.; Sillescu, H. *J. Magn. Reson.* **1981**, *42*, 381.
(72) Vega, A. J.; Luz, Z. *J. Chem. Phys.* **1987**, *86*, 1803.
(73) Wittebort, R. J.; Szabo, A. *J. Chem. Phys.* **1978**, *69*, 1722.
(74) Freed, J. H. *J. Chem. Phys.* **1977**, *66*, 4183.